Resonance Raman Spectroscopy to Study and Characterize Defects on Carbon Nanotubes and other Nano-Graphite Systems

Ado Jorio,[1] Luiz Gustavo Cançado,[1] Bernardo R. A. Neves,[1] Mauricio de Souza,[1] Cristiano Fantini,[1] Marcos A. Pimenta,[1] G. Medeiros-Ribeiro,[3] Georgii G. Samsonidze,[2] Shin Grace Chou,[4] Gene Dresselhaus,[5] Mildred S. Dresselhaus,[2, 6] A. M. Rao,[7] Alexander Grüneis,[8] and Riichiro Saito[8]

[1] Depto. de Física, Universidade Federal de Minas Gerais, Belo Horizonte, Minas Gerais, Brazil.
[2] Dept. of Electrical Engineering and Computer Science, MIT, Cambridge, MA, USA.
[3] Laboratório Nacional de Luz Síncrotron, Campinas, São Paulo, Brazil.
[4] Dept. of Chemistry, MIT, Cambridge, MA, USA.
[5] Francis Bitter Magnet Laboratory, MIT, Cambridge, MA, USA.
[6] Dept. of Physics, MIT, Cambridge, MA, USA.
[7] Dept. of Physics and Astronomy, Clemson University, South Carolina 29634, USA
[8] Dept. of Physics, Tohoku University and CREST JST, Sendai, Japan.

ABSTRACT

The use of resonance Raman spectroscopy (RRS) to study and characterize single wall carbon nanotubes (SWNTs) is discussed, focusing on preliminary efforts for the development of the RRS to characterize defects in SWNTs. The disorder-induced D-band, disorder-induced peaks just above the first-order allowed graphite G-band, as well as the intermediate frequency modes (IFMs) appearing between the RBM and the D/G spectral region are addressed. RRS on nanographite ribbons and on a step-like defect in highly ordered pyrolytic graphite (HOPG) sheds light into the problem of characterizing specific defects in nano-related carbons.

INTRODUCTION

Major effort has been made to develop the nanotechnology based on single wall carbon nanotubes (SWNTs) [1]. Some of the big challenges for the development of SWNT nanodevices are the selective (*n,m*) growth, SWNT manipulation, tube-metal contacts, tube-tube junctions, tube functionalization. While microscopic techniques are largely used for characterization of specific structures for a given (*n,m*) nanotube, the development of spectroscopic techniques has been shown to be very effective for simple, quick, cheap and non-destructive characterization of SWNT properties. Photoluminescence (PL) [2] and resonance Raman spectroscopy (RRS) [3] have been developed at the single SWNT level and are now largely used to characterize the population of (*n,m*) SWNTs in a sample. RRS has the advantage of studying both electrons and phonons, and gives information about the presence of defects and impurities in the samples [4].

While RRS is well established to determine the properties of a perfect SWNT, the ability of this technique to characterize defects is still poorly developed [3,4]. The big challenge for researchers working with RRS on SWNTs is the development of the RRS technique for the characterization of specific defects in a given (*n,m*) tube. By *defects* we mean any structure that modifies the perfect atomic structure of a nanotube, but useful for device production. In this

paper we describe our preliminary efforts to make RRS a tool able to characterize specific defects on a given (*n,m*) SWNT. To achieve this goal, much work will be necessary. We start by discussing the spectroscopic effect of the most simple defect structures on the simple material graphite, that is the end of a graphite basal plane, i.e. a graphite step, and a nanographite ribbon. From the other extreme, we discuss what is known about the spectroscopy of defects in SWNTs, calling attention to a poorly studied spectral region of carbon nanotubes that is promising for providing rich information about specific defect structures in SWNTs.

EXPERIMENTAL DETAILS

We present RRS results on SWNTs grown by the arc process [1], as well as B doped SWNTs [5]. We also present results on nanographite ribbons and graphite steps. The RRS experiments are made at room temperature and pressure, using a Dilor XY triple monochromator with a N-cooled charge couple device (CCD) detector and a microscope. Scanning probe microscopy measurements were performed with a Veeco Nanoscope IV MultiMode microscope.

DISCUSSION

The Raman spectroscopy of edges in graphite

Phonons in SWNTs are very closely related to phonons in 2D graphite [3]. The understanding of the spectroscopic signature of defects in a graphene sheet is, therefore, one good path to learn about nanotubes. A very simple defect in a 2D graphene sheet is the end of the sheet, giving a step on 3D graphite. The bounding edge of the graphene sheet can exhibit armchair, zigzag or any atomic orientation in between, being either a strait perfectly uni-dimensional defect, or an imperfect fractal edge, like a seacoast.

We measured the Raman spectra of several graphite steps, and studied the intensity of the well-known defect-related D band. This band is known to appear in the Raman spectra of graphite-like materials only when defects are present in the lattice, so that the translation symmetry is broken and phonons in the interior of the Brillouin zone can be observed in a Raman scattering process. Interestingly, we observe that the D-band intensity varies strongly from step to step. Particularly, it is sometimes very weak when measuring edges with a predominant zigzag structure.

Figure 1-top shows an atomic force microscopy (AFM) image of a graphite step. Although we are not able to atomically characterize a large spot at the step edge, the preferential ordering of the atoms at the step can be characterized by scanning tunneling microscopy (STM) close to the step edge. A preferential zigzag atomic ordering in the step is obtained from STM in Fig.1-top. Figure 1-bottom shows the Raman spectra at two spots on different step edges: a border with armchair preferential structure (Point 1); the step edge shown in Fig.1(a), with zigzag preferential atomic structure (Point 2). While the first-order Raman-allowed G band exhibits the same intensity in all the spectra, the disorder-induced D band is stronger in the armchair-like step edges and weaker in zigzag-like step edges (with respect to the G band). Some Raman spectra on other zigzag-like step edges show larger D-band features when compared to the spectrum shown in Fig.1-bottom (Point 2), but never larger than the D-band for the armchair-like step edge.

The D-band scattering involves a double resonance process that would be forbidden for a perfect zigzag edge structure [6]. The analysis of the D-band intensity on a graphite edge, therefore, is related to the ordering of the atoms at the step edge, depending both on the armchair vs. zigzag preferential atomic ordering, and on the one-dimensional (1D) perfection of the step edge. The D-band intensity on graphite edges depend on the light polarization direction, as described in Ref. [6].

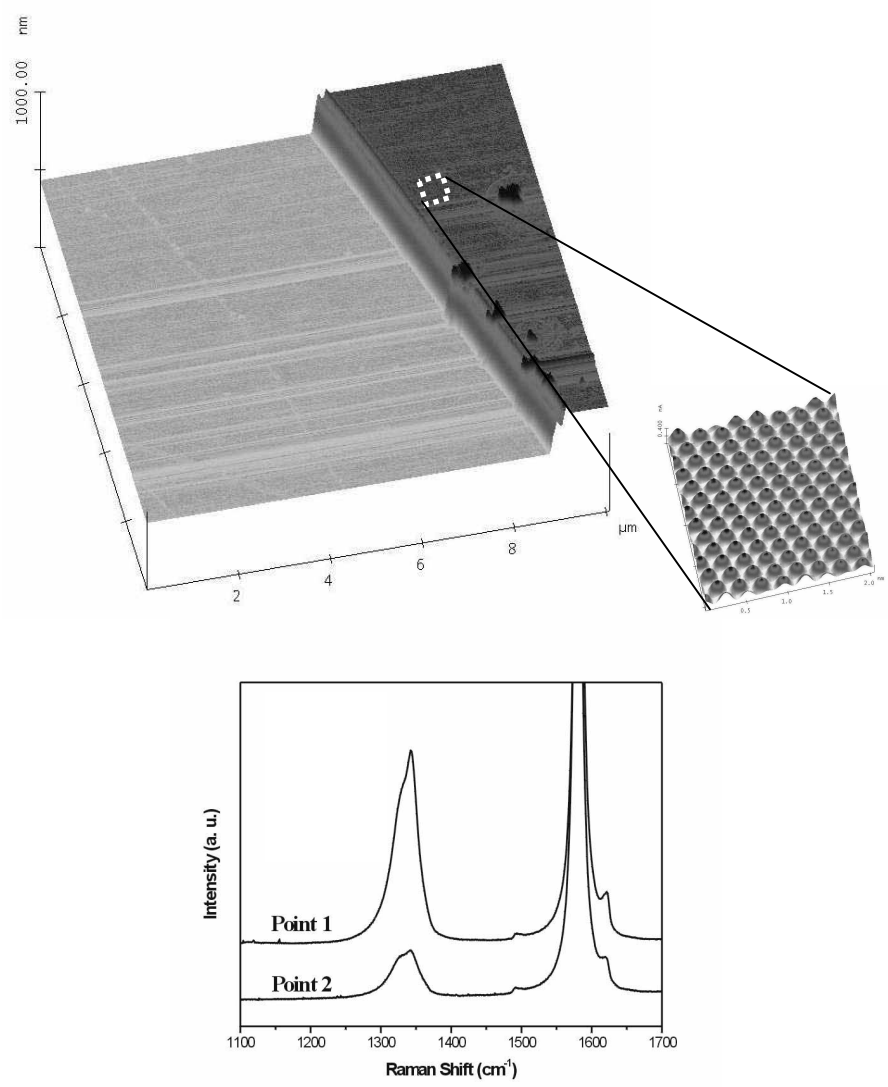

Figure 1. Top - AFM image of a graphite edge. The STM image close to the edge shows that the atoms at the edge exhibit preferentially a zigzag ordering. Bottom - Raman spectra at two points on different step edges: Point 1 – edge with a preferentially armchair atomic structure. Point 2: the step edge shown in (a), with a zigzag preferential structure. The 514nm laser line was used.

The Raman spectroscopy of nanographite ribbons

If we have edges limiting the graphene sheet at both sides, we have the formation of a nanographite ribbon. Figure 2-left shows AFM and STM images of nanographite ribbons on an

HOPG substrate. The smaller nanographite ribbon has a 1nm height, equivalent to 3 graphene layers. The G band of the nanographite ribbon can only be measured with high laser power. Since the heat dissipation is less efficient in the nanographite ribbon, the ribbon will be heated to a higher temperature than the graphite substrate and the G band will be observed at a lower frequency (see Fig.2-right). Interestingly, the Raman spectra of the nanographite ribbon can only be observed if the light is polarized parallel to the ribbon axis, being absent when the light is polarized perpendicular to the axis. This polarization effect is explained by the anisotropy of the optical absorption in graphite combined with the 1D nature of the ribbon [7].

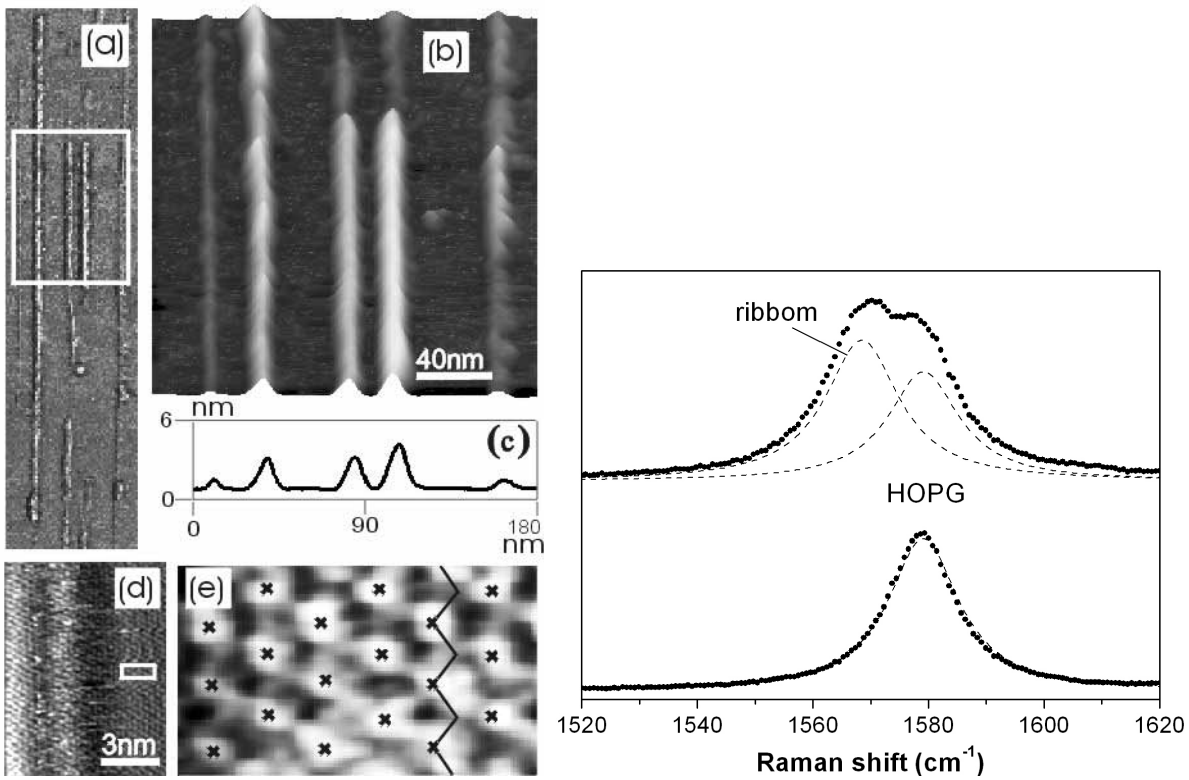

Figure 2. Left - (a) AFM image of a set of nanographite ribbons. (b) Magnification of image (a). (c) height profile for (b). (d) STM image of a nanographite ribbon. (e) Magnified image from the white rectangle in (d), showing a zigzag atomic structure along the ribbon axis. Right - G band Raman spectra of the nanographite ribbon sitting on a graphite substrate for light polarized along the ribbon axis (top) and perpendicular to the ribbon axis (bottom). The 514nm laser line was used.

The spectroscopy of defects in SWNTs and the Intermediate Frequency Modes

The presence of disorder-induced peaks in the Raman spectra of graphite-like materials, including SWNTs, is well known. Although the most common disorder-induced feature is the D band, many features can be induced by defects in the entire spectral region that goes up to 1620cm^{-1}. Recently it was shown that the G band exhibits a larger number of peaks at the edge of a SWNT fiber, where defects are expected to be abundant (see Fig.3(a)) [8].

Besides these well known features, the frequency region between the first-order radial breathing modes (RBMs, usually between 100-450cm^{-1}) and the D-G bands (~1250-1620cm^{-1}) was also shown to be very rich in Raman features [3,9-11]. Figure 3(b) show the intermediate frequency modes (IFMs) for a pristine (top) and a B doped (bottom) SWNT bundles sample, and the spectra are very different. The frequencies for these features in pristine SWNTs have been explained based on the double resonance model developed for the D band in graphite [12]. This model, when extended for the many features observed in graphite-like materials [13], shows how phonons from the interior of the 2D graphite Brillouin zone are selected by a resonance scattering process to become effectively observed in a second-order Raman scattering process.

Although the double resonance model has been successful to explain the frequencies observed for the disorder-induced peaks in SWNTs [14], it has up to now not been related to the specific structure of the defect. The only assumption that is made is the presence of a defect to break the translation symmetry. If the defect is a vacancy, a 7-5 pair, or a metallic contact, it is not an issue for the model. These considerations are expected to be important when analyzing the intensity of the defect-induced scattering processes, as shown for the defect induced scattering at the step edge of a graphite plane (see section "The Raman spectroscopy of edges in graphite" above). Theoretical works [15,16] predict that the intensity of the rich set of Raman features in the intermediate frequency modes region will depend on the size of the tube. Likely the relative intensities will depend not only on size of the tube, but also on the distance between defects, between contacts, or on the presence of any structure that could effectively limit the size of the tube.

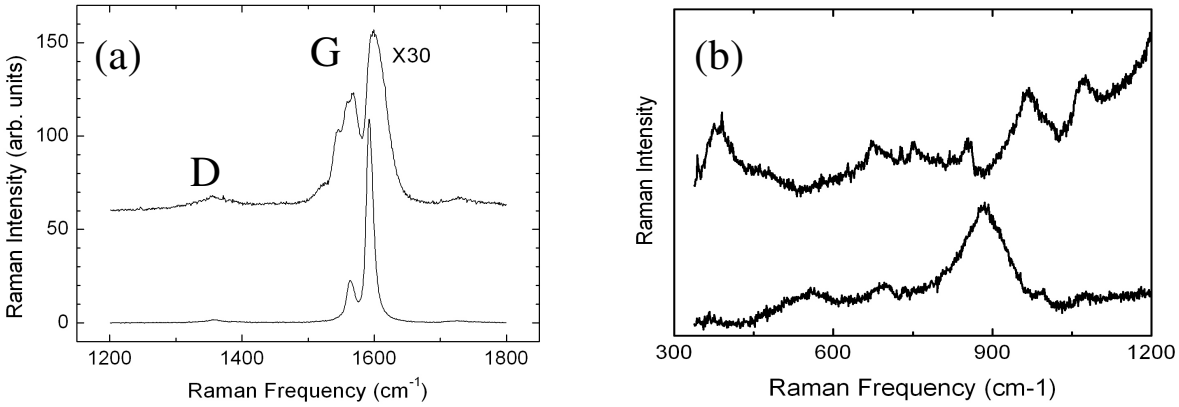

Figure 3. (a) D and G band spectra of a SWNT-PMMA fiber [8] with E_{laser} = 2.71eV. The lower spectrum was obtained at the center of the fiber, where the tubes are well aligned. The top spectrum was obtained at the edge of the fiber, where defects are expected to be abundant. (b) Raman spectra of the intermediate frequency modes (IFMs) with E_{laser} = 2.41eV. The top spectrum comes from a pristine SWNT sample grown by the arc process. The bottom spectrum comes from a B doped SWNT sample.

CONCLUSIONS

In this work we propose routes for the development of the resonance Raman scattering to become a spectroscopic tool for the characterization of defects in carbon nanotubes. We call attention to the richness of information contained in the Raman spectra of SWNTs, that has been

poorly studied in the past, but is promising for providing detailed information about specific structures in an imperfect nanotube crystal. For example, we show that the intensity of the well-known D band Raman feature observed at the step edge of a graphene sheet depends on the atomic ordering of the edge. Furthermore, the IFMs change significantly from pristine SWNTs to B doped SWNTs. These results indicate that with future theoretical and experimental effort, the development of spectroscopic signatures of specific defects in carbon nanotubes will be possible.

ACKNOWLEDGEMENTS

A.J. acknowledge financial support from FAPEMIG and CNPq. MIT authors acknowledge support under NSF Grants DMR 04-05538 and INT 00-00408. R.S. and A.G. acknowledge a Grant-in-Aid (No. 13440091) from the Ministry of Education, Japan. Some STS/STM measurements were performed at the Laboratório Nacional de Luz Sincrontron, Brazil.

REFERENCES

1. M. S. Dresselhaus, G. Dresselhaus and Ph. Avouris, in *Carbon Nanotubes: Synthesis, Structure, Properties and Applications* (Springer Series in Topics in Appl. Phys., Springer-Verlag, Berlin, 2001).
2. S. M. Bachilo, M. S. Strano, C. Kittrell, R. H. Hauge, R. E. Smalley, and R. B. Weisman, *Science* **298**, 2361 (2002).
3. A. Jorio, M. A. Pimenta, A. G. Souza Filho, R. Saito, G. Dresselhaus, and M. S. Dresselhaus, *New Journal of Physics* **5**, 1.1 (2003). M. S. Dresselhaus, G. Dresselhaus, A. Jorio, A. G. Souza Filho, and R. Saito, *Carbon* **40**, 2043 (2002).
4. A. G. Souza Filho, A. Jorio, Ge. G. Samsonidze, G. Dresselhaus, R. Saito, and M. S. Dresselhaus, *Nanotechnology* **14**, 1130 (2003).
5. M. Terrones, A. Jorio, M. Endo, A. M. Rao, Y. A. Kim, T. Hayashi, H. Terrones, J.-C. Charlier, G. Dresselhaus, and M. S. Dresselhaus, *Materials Today* **7**, 30 (2004).
6. L. G. Cançado, M. A. Pimenta, A. Jorio, R. A. Neves, G. Medeiros-Ribeiro, T. Enoki, Y. Kobayashi, K. Takai, K. Fukui, M. S. Dresselhaus, and R. Saito, *Phys. Rev. Lett.* **93**, 047403 (2004).
7. L. G. Cançado, M. A. Pimenta, B. R. A. Neves, M. S. S. Dantas, and A. Jorio, *Phys. Rev. Lett.* In press.
8. M. Souza, A. Jorio, C. Fantini, B. R. A. Neves, M. A. Pimenta, R. Saito, A. Ismach, E. Joselevich, V. W. Brar, Ge. G. Samsonidze, G. Dresselhaus, and M. S. Dresselhaus, *Phys. Rev. B* **69**, R241403 (2004).
9. L. Alvarez, A. Righi, S. Rols, E. Anglaret and J. L. Sauvajol, *Chem. Phys. Lett.* **320**, 441 (2000).
10. C. Fantini, A. Jorio, M. Souza, L. O. Ladeira, M. A. Pimenta, A. G. Souza Filho, R. Saito, Ge. G. Samsonidze, G. Dresselhaus and M. S. Dresselhaus, *Phys. Rev. Lett.* **93**, 087401 (2004).
11. H. Son, Y. Hori, S. G. Chou, D. Nezich, Ge. G. Samsonidze, G. Dresselhaus, M. S. Dresselhaus, and E. Barros, *Appl. Phys. Lett.* **85**, 4744 (2004).
12. C. Thomsen and S. Reich, *Phys. Rev. Lett.* **85**, 5214 (2000).
13. R. Saito, A. Jorio, A. G. Souza Filho, G. Dresselhaus, M. S. Dresselhaus, and M. A. Pimenta, *Phys. Rev. Lett.* **88**, 027401 (2002).
14. R. Saito, A. Grüneis, Ge. G. Samsonidze, V. W. Brar, G. Dresselhaus, M. S. Dresselhaus, A. Jorio, L. G. Cançado, C. Fantini, M. A. Pimenta, and A. G. Souza Filho, *New Journal of Physics* **5**, 157 (2003).
15. R. Saito, T. Takeya, T. Kimura, G. Dresselhaus, and M. S. Dresselhaus, *Phys. Rev. B* **59**, 2388 (1999).
16. A. Rahmani, J.-L. Sauvajol, S. Rols, and C. Benoit, *Phys. Rev. B* **66**, 125404 (2002).